

Morphology and Structure of Carbon Films Deposited at Varying Chamber Pressure

Mubarak Ali^a *, Mustafa Ürgen^b

^aDepartment of Physics, COMSATS University Islamabad, Islamabad Campus, 45550, Park Road, Pakistan, *mubarak74@mail.com, <http://orcid.org/0000-0003-1612-6014>

^bDepartment of Metallurgical and Materials Engineering, Istanbul Technical University, 34469 Maslak, Istanbul, Turkey, E-mail: urgen@itu.edu.tr

Abstract: Depositing carbon films by a hot-filament CVD technique is an area of great interest. A carbon film is deposited at some value of the chamber pressure, depending on the composition of gases. In the hot-filament reactor, having dissociated from methane precursor, gaseous carbon atoms first convert into the graphite state atoms and then into the diamond state atoms. An increase in the chamber pressure changes the morphology and structure of the deposited carbon films. The growth rate of the deposited carbon film increases by increasing the chamber pressure from 3.3 kPa to 8.6 kPa. The rate of converting gaseous carbon atoms into diamond state atoms also increases. At 11.3 kPa and 14 kPa high chamber pressures, gaseous carbon atoms converted into the graphite state atoms at a high rate. However, the films with low growth rates are deposited. The gas activation and gas collision processes vary broadly at varying chamber pressure. Hence, the morphology and structure of carbon films got deposited with different nucleation and growth rates. The rate of dissociating molecular hydrogen into atomic hydrogen becomes different for a different chamber pressure. Atomic hydrogen is used to etch the photons emitted from hot filaments converting them into typical energy of different shapes. The amount of formation of typical energy varies at varying chamber pressure. Certain-shaped typical energy converts the gaseous carbon atoms into the graphite and diamond state atoms. Graphite state atoms get bound by the previously involved typical energy. However, a different shaped typical energy is involved in the process of binding diamond state atoms. The study sets a new trend in depositing, characterizing, and analyzing the carbon films.

Keywords: Chamber pressure; Carbon films; Morphology and Structure; Photon energy; Materials Chemistry; Analytical Chemistry

1.0. Introduction

By employing different vapor deposition systems, many research groups generally deposited graphite and diamond-based films related to carbon films. In addition to studying different parameters, the chamber pressure was also considered in the studies. Some studies show the handling of deposition at low chamber pressures. Some studies show the selection of high chamber pressures.

Among the various techniques, hot-filament chemical vapor deposition (HF-CVD) was considered suitable for synthesizing carbon films. HF-CVD is simple for synthesizing carbon films. Many studies suggest various aspects of carbon films, including their quality and growth rate [1-8]. Carbon films in higher diamond content discussed some exciting aspects [9-14]. In the deposition of carbon films, switching dynamics under different conditions have been discussed [6]. It has also been pointed out that the low growth rate of diamond film in HF-CVD has been the main drawback of the technique compared to the flame jet technique [15]. The HF-CVD technique deposited a uniform layer of thickness of around 40 μm [16].

A key parameter in the CVD diamond process is the system pressure, as it regulates the overall features of a carbon film. A systematic study on the influence of chamber pressure in depositing carbon films is not executed. Studies have reported that diamond film deposited at a low pressure contained more non-diamond components than those deposited at high pressure [17, 18]. Kang *et al.* [18] deposited well-faceted diamond cubes over silicon by keeping the chamber pressure at nucleation stage 0.13 kPa and chamber pressure raised to 2.7 kPa during the growth period. Yu and Flodström [19] observed that diamond {100} is a favorable growth surface at higher pressure, whereas diamond {111} is a favorable growth surface at lower chamber pressure.

Heimann *et al.* [20] studied the influence of pressure, deposition time, and mean residence time, where sufficient amounts of diamond were deposited at chamber pressures 4 kPa and 20 kPa, but not at chamber pressures 0.8 kPa and 40 kPa. The growth rate of the carbon film at a chamber pressure of 200 kPa was about four times

higher than the carbon film deposited at a chamber pressure of 50 kPa [21]. The set residence time also affects the growth rate [21, 22]. When the diamond films were deposited at cemented carbide substrates, a faceted morphology was obtained at 1.3 kPa, and 2.7 kPa chamber pressures, whereas poor crystallinity was obtained at 0.7 kPa and 6.7 kPa chamber pressures [23]. The growth rate of diamond film was increased between 1.2 kPa and 2.7 kPa [24]. Wan *et al.* [25] found that CVD diamond synthesis is restricted by the gas phase composition and the temperature and pressure. Brunsteiner *et al.* [26] investigated the dependence of the growth rate on chamber pressure and found the maximum growth rate at chamber pressure was 2.7 kPa.

The deposition of carbon films can emerge with several applications. When the deposited carbon films are in the high-quality diamond phase, they can work efficiently for abrasive, cutting tools, and heat sink applications. When the deposited carbon films are rich in graphite phase, they can work efficiently for electrode and field emission applications. When the deposited carbon films are equally good in diamond and graphite phases, they can work efficiently for the hybrid application.

The chamber pressure in depositing carbon films by the HF-CVD system is considered a critical parameter. There is incomplete information explaining the underlying science of deposited carbon films. Hot filaments not only convert molecular hydrogen into atomic hydrogen but also release photons. The atomic hydrogen does not etch carbon, but atomic hydrogen is used to etch photon energy into the typical energy.

Despite different opinions on the results of some research groups, the discussion based on the science of influencing chamber pressures to deposit carbon films strikingly demands a comprehensive study, which can provide a new foundation to discuss the nucleation and growth mechanisms. The influence of chamber pressures in depositing carbon films is investigated in this study by carrying the same aim. Deposition of carbon films has been conducted at some appropriate chamber pressures. The morphology and structure of deposited carbon films have been discussed in the light of X-ray reflection and microscopic and spectroscopic analyses.

2.0. Experimental Details

Different experiments were performed to deposit the carbon films by employing an HF-CVD system. In the deposition of carbon films, filaments of the tantalum wire were made by winding it in 16 parallel wires. The diameter of the wire is 0.5 mm, and the length of the wire is 13 cm. The distance between the substrate and filaments was set at ~ 7 mm. The distance between the wires was set at ~ 10 mm.

The base pressure was set around 3×10^{-3} Pa. A molecular turbopump maintained the base pressure. The vane pump-2 was used to drain the gaseous species and maintain the deposition pressure for each set value. The vane pump-2 was also used to maintain the set value of the chamber pressure. This study studied the influence of varying chamber pressure from 3.3 kPa to 14 kPa. In each experiment, the total mass flow rate of the H₂ and CH₄ mixture was set at 304.5 sccm. Built-in mass flow controllers controlled the flow of H₂ and CH₄ gases. The methane concentration for each experiment was set at 1.5%. The approximate volume of the chamber was 2.9 cubic ft. The different parameters chosen in the depositions of carbon films are given in Table 1.

Table 1: Parameters of depositing carbon films at varying silicon substrates

Chamber pressure (kPa)	Filament temperature (°C)	Current (in amp)/ voltage (in volts)	Substrate Temperature (°C)	Flow rate of gases (sccm)
3.3	2100	255/12	895	CH ₄ : 4.5, H ₂ : 300
6.0	2050	255/14	880	CH ₄ : 4.5, H ₂ : 300
7.3	2030	255/16	905	CH ₄ : 4.5, H ₂ : 300
8.6	2030	255/14	925	CH ₄ : 4.5, H ₂ : 300
11.3	1800	255/12	820	CH ₄ : 4.5, H ₂ : 300
14.0	1765	255/12	795	CH ₄ : 4.5, H ₂ : 300

The temperature of the hot filaments was maintained at an input power of ~ 3.3 kW. At each chamber pressure, the temperature of the substrate was recorded at an approximate value. The temperature of the substrates was maintained by heating of filaments. Both optical pyrometer and K-type thermocouple were used to measure the temperature. The rotational speed of the substrate holder was set at 5 rpm, and ten hours of processing time was set in each experiment. An initial 13 min was spent to reach the set chamber pressure.

Polished p-type (100) silicon substrates (area 2×2 cm² and thickness 400 μm) were agitated ultrasonically. Before that, substrates were mechanically scratched for 5 minutes with suspension. The suspension was prepared with diamond powder having mesh size ~ 30-40 (~ 28 μm) and acetone. The silicon samples were again scratched for 10 minutes by another suspension. The suspension was prepared with acetone and diamond powder having an average size of a grain of 5 μm. After the step, the samples were washed with acetone to remove any debris from the substrate. The adoption of the lengthy seeding treatment is to enhance the nucleation rate. The samples were placed on 2 cm thick molybdenum supported by 8.0 mm alumina boats. They were placed all together in the copper holder, and fresh filaments were prepared in each experiment.

The X-ray reflectometer determined structural regularity in different carbon films (Philips PW3710). A copper line focusing X-ray tube producing K α radiation in wavelength 1.541874 Å was used. The X-ray reflectometer is conventionally known as an X-ray diffractometer. The field-emission scanning optical microscope performed the morphology and interface studies, FE-SOM (JEOL Model: JSM-7000F). The FE-SOM is conventionally known as FE-SEM. Carbon films were analyzed by micro-Raman spectroscopy (HR800 UV; 632.8 nm, He-Ne Red Laser).

3.0. Results and Discussion

3.1. Structural Examination of Carbon Films by X-ray Analysis

Patterns of the carbon films deposited at varying chamber pressure are shown in Figure 1 (a-f). Carbon films show the peaks at $2\theta \sim 43.9^\circ$, $\sim 75.3^\circ$, $\sim 91.5^\circ$, and $\sim 119.5^\circ$. Peaks are conventionally related to the (111), (220), (311), and (400) planes. The peak at $2\theta \sim 43.9^\circ$ is now labeled by D (OR-R), related to diamond outer ring electrons reflection. The peak at $2\theta \sim 75.3^\circ$ is now labeled by D (ZR-R), related to the diamond zeroth ring electrons reflection. The peak at $2\theta \sim 91.5^\circ$ is now labeled by D (ZR-IR), related to the diamond zeroth ring electrons inverse reflection. The peak at $2\theta \sim 119.5^\circ$ is now labeled by D (OR-IR), related to the diamond outer ring electrons inverse reflection.

The peaks related to the carbon films show both diamond and graphite phases. At chamber pressures 11.3 kPa and 14.0 kPa, X-ray analyses of carbon films show a high

regularity of structure in the graphitic phase. The pronounced peak at $2\theta \sim 56.1^\circ$ in Figures 1 (a) and 1 (d-f) is related to the graphitic phase of the carbon film. The peak at $2\theta \sim 56.1^\circ$ has a very high intensity in carbon films deposited at chamber pressures of 11.3 kPa and 14.0 kPa, indicating the deposition of carbon films in the highly-graphitic phase. The peaks related to the diamond phase are almost diminished in the patterns of carbon films deposited at 11.3 kPa and 14.0 kPa. In Figure 1, the peak at $2\theta \sim 56.1^\circ$ is related to the graphite (zeroth ring-reflection). It is designated by G (ZR-R).

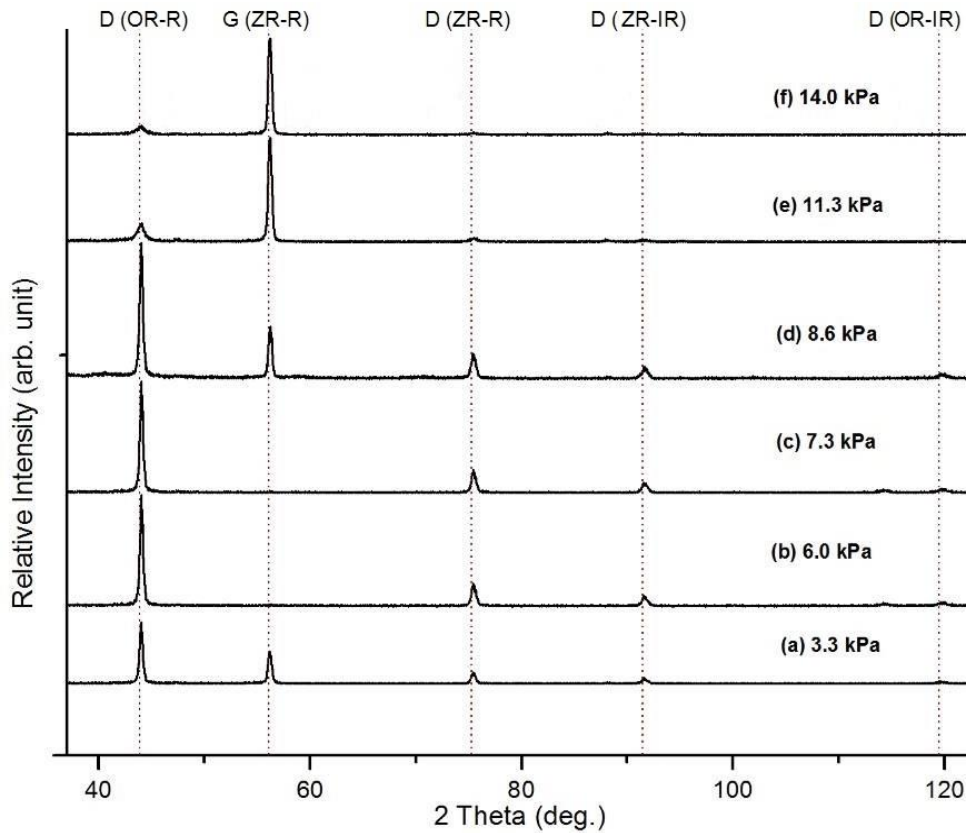


Figure 1: Structural determination of carbon films deposited at different chamber pressures, GIA = 0.5°

The peaks found in different patterns are related to the interaction of X-rays with atomic electrons of grains and particles belonging to the top-layered surface of carbon films. At chamber pressures, 6.0 kPa and 7.3 kPa, the peak at $2\theta \sim 56.1^\circ$ is nearly diminished. The less-intensive graphitic peak appears in the patterns of carbon films deposited at the chamber pressures of 3.3 kPa and 8.6 kPa. From the top-layered surface exposed to X-rays, the structural regularity in terms of the diamond phase is the

highest in carbon film synthesized at the chamber pressure of 7.3 kPa. In Figure 1 (d), the film deposited at 8.6 kPa chamber pressure shows the highest intensity peak at $2\theta = 43.9^\circ$. However, the deposited film also indicates the peak of a graphite phase at $2\theta \sim 56.1^\circ$.

The carbon phases other than graphite and diamond can be found in the deposited carbon films. Such clusters of carbon atoms can develop amorphous carbon, containing only a few atoms. The clusters of amorphous carbon structure can also contain diamond state atoms or atoms of other carbon states. So, the atoms of diamond and graphite can be found in an amorphous carbon phase, but they do not record the intensity of the reflecting X-rays due to minor effects and details. However, reflected X-rays from the tiny grains, grains, and particles containing a diamond phase or a graphite phase print the associated peaks in the X-ray reflection (XRR) pattern. Further detail on a structural determination by XRR analysis is given elsewhere [27].

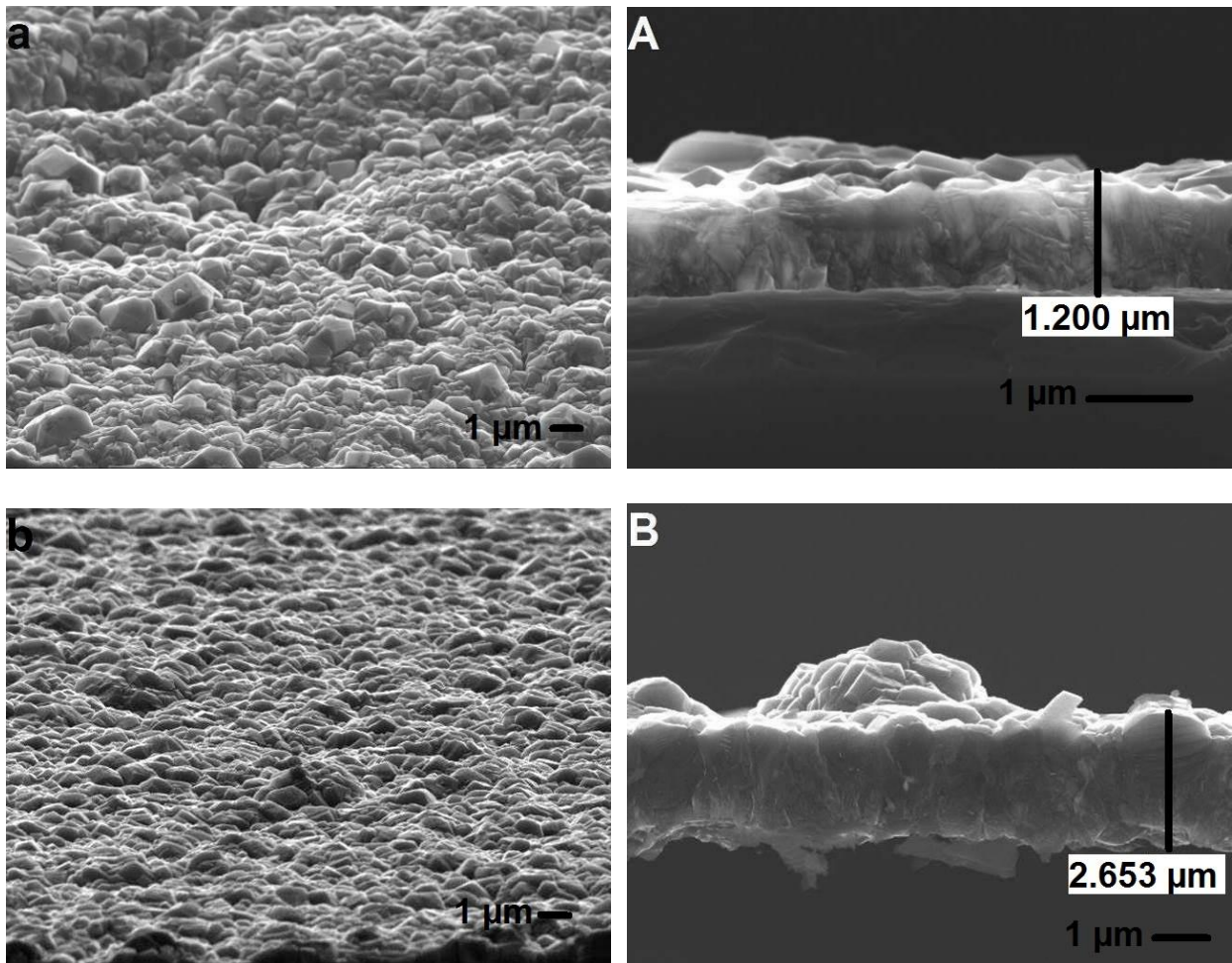
3.2. Surface Morphology and Interface Study of the Carbon Films

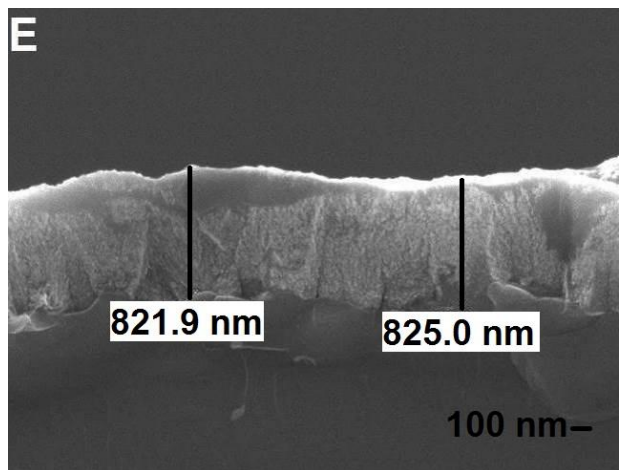
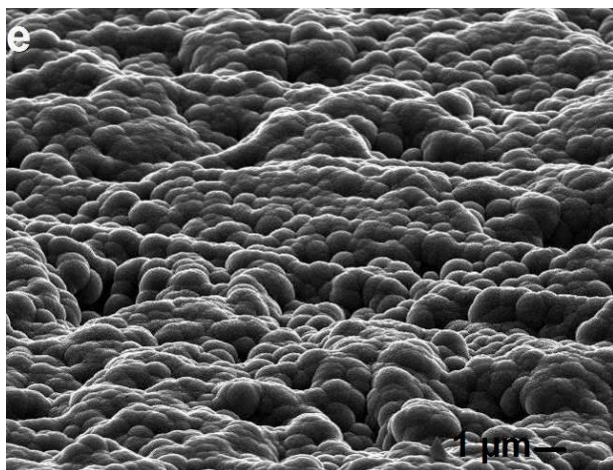
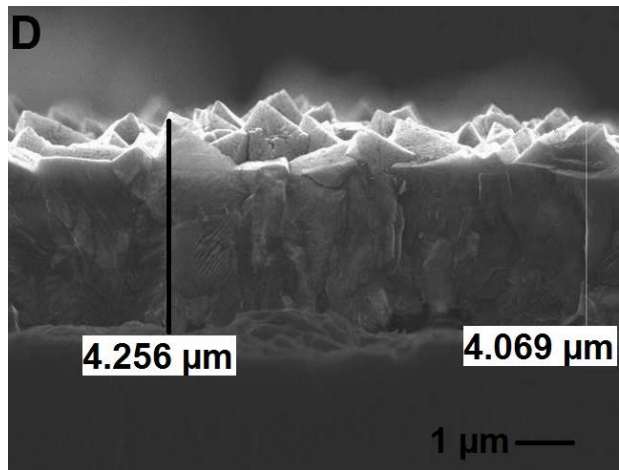
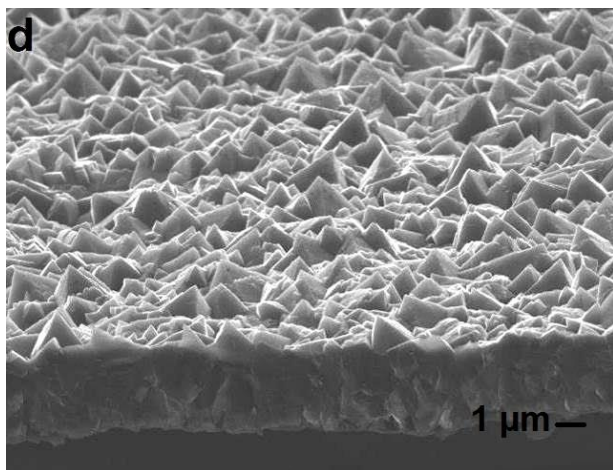
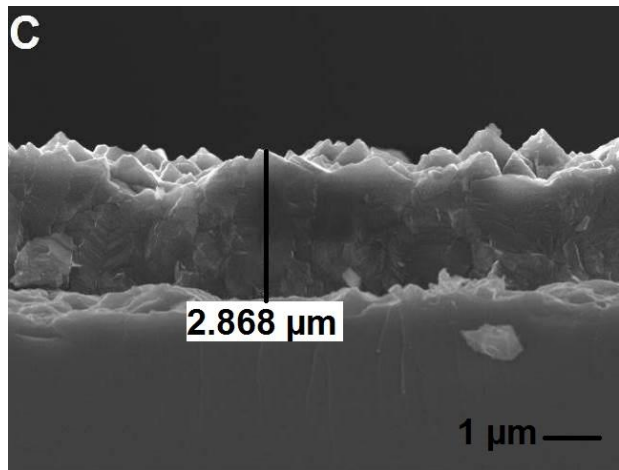
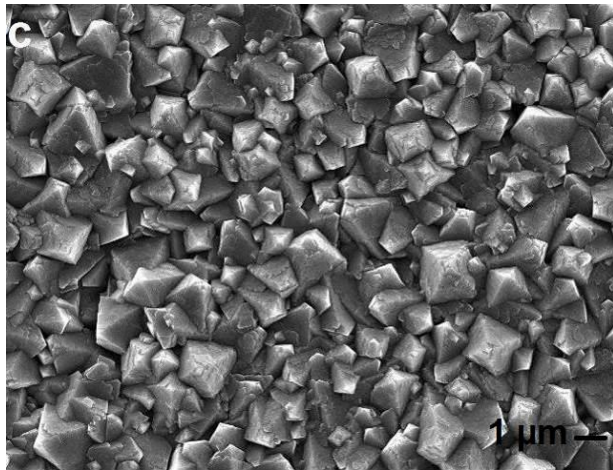
The carbon film grows uniformly at the lowest chamber pressure, 3.3 kPa. Figure 2 (a) shows that the deposited carbon film contains tiny grains, grains, and particles. The morphology of the carbon film shows uniform distribution of tiny-sized grains, grains, and particles. Some grains and particles grow with the smooth faces in the carbon film. Many grains and particles also show their non-uniform growth behaviors. Due to the sharp edges of the crystallites, their growth shows different faces. Many crystallites were also grown with broken faces. In the case of the fractured cross-sectional image of the carbon film, shown in Figure 2 (A), the growth behavior of different-sized grains is almost similar to that shown in the surface view. Some grains and particles grow with the broken faces at the upper side of the interface. Many nucleated tiny-sized grains do not grow further, as shown in Figure 2 (A). Thus, new tiny grains started nucleating.

At chamber pressure of 6.0 kPa, the dynamics of carbon atoms become favorable to grow tiny-sized grains and grains into the size of particles. Figure 2 (b) shows that the morphology of tiny grains, grains, and particles deviated toward the cubic growth behavior. In Figure 2 (B), a cubic growth behavior was more evident. The growth rate doubled when the carbon film was deposited at a chamber pressure of 6.0 kPa. In

Figure 2 (B), the growth of a very large-sized particle is also found. Grains and particles were amalgamated in one region at a very high rate, as shown in Figure 2 (B). A particle is related to the size in the submicron range, but a crystallite is related to the shape.

At chamber pressure of 7.3 kPa, the growth behavior of grains and particles was in pyramid-shaped morphology, and many tiny-sized grains increased the size to reach up to the size of particles and started growing from the nucleated points in contact with the substrate. Later, grains and particles attained uniformity in the growth behavior, as shown in Figure 2 (c). A uniform growth rate of carbon film was attained because the temperature remained constant. The pyramid-shaped grains and particles nucleated at the start of the process, as shown in Figure 2 (C).





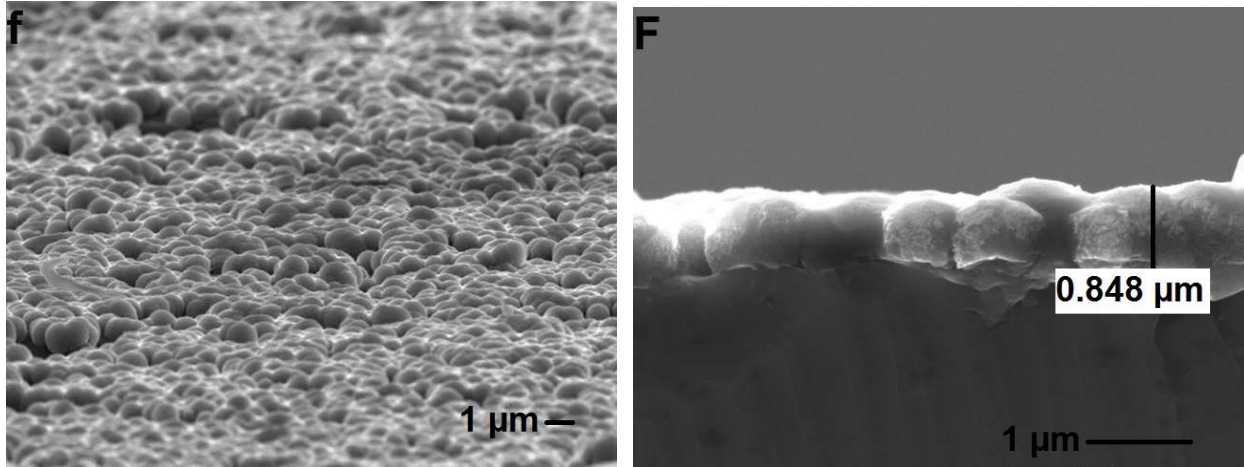


Figure 2: Surface morphology and fractured cross-sectional images of carbon films deposited at chamber pressure (a) 3.3 kPa, (b) 6.0 kPa, (c) 7.3 kPa, (d) 8.6 kPa, (e) 11.3 kPa and (f) 14.0 kPa

At chamber pressure of 8.6 kPa, growth behavior is more dominant in the pyramid-shaped morphology of grains and particles. It is shown in the tilted-positioned image of the film in Figure 2 (d). The morphology of grains and particles develops from the surface of the substrate, which could also be verified from the fractured cross-sectional view of the carbon film, as shown in Figure 2 (D). Initially, grown grains and particles are nucleated from the roughened substrate surface.

At chamber pressure 11.3 kPa, grains and particles grow in shape like domes. Many grains and particles were connected from the sides in the growing competition. So, a process of secondary nucleation was initiated in the growing film. Tiny-sized grains started growing in the left spaces of irregularly grown particles, as shown in Figure 2 (e). This behavior is evident in the fractured cross-sectional view of the carbon film, as shown in Figure 2 (E). The thickness of the carbon film synthesized at chamber pressure 11.3 kPa decreased several times compared to the carbon film deposited at chamber pressure 8.6 kPa. The thickness of the carbon film is even less than that of the carbon film deposited at a chamber pressure of 3.3 kPa. As labeled in the fractured cross-sectional view, thickness is less than one micron, as shown in Figure 2 (E).

In Figure 2 (f), grains and particles grow in dome shapes. In the carbon film, grains and particles are uniformly dispersed. The thickness of the carbon film deposited at chamber pressure 14.0 kPa is almost the same as in the case of a carbon film deposited at chamber pressure 11.3 kPa. The labeled thicknesses keep slightly different

values in the fractured cross-sectional views of the carbon films shown in Figures 2 (E) and 2 (F).

The substrate temperature reached 1100 °C at increasing the chamber pressure from 5.3 kPa to 39.5 kPa, and the morphology of the carbon film got varied, as discussed elsewhere [20]. However, the primary mechanism of the change of morphology remained unclear. The average crystal size of the diamond was 0.3 μm, 2 μm, and 1 μm at chamber pressures of 0.3 kPa, 2.0 kPa, and 5.0 kPa, respectively, and it was identified by Schwarz *et al.* [22]. Schwarz *et al.* [22] observed the pressure-dependent growth rate of diamond coatings at substrate temperature 850 °C; the growth rate was maximum (0.7 μm/h) at chamber pressure 0.3 kPa and reached the minimum value (0.1 μm/h) at chamber pressure 2.0 kPa. On the other hand, the growth rate was 0.2 μm/h at a chamber pressure of 5.0 kPa. A bit lower growth rate was recorded at a chamber pressure of 0.7 kPa in the study given elsewhere [26].

At low chamber pressures, our results agree reasonably with the chamber pressures 2.0 kPa to 5.0 kPa as given elsewhere [22]. From chamber pressure 6.7 kPa to 67 kPa, the deposition rate was decreased by increasing the gas pressure. At the highest value of the chamber pressure, the growth rate decreased below 0.05 μm/h [26]. However, in the present study, the highest growth rate (~ 0.4 μm/h) was obtained at a chamber pressure of 8.6 kPa, which drastically decreased at chamber pressures of 11.3 kPa and 14.0 kPa (~ 0.1 μm/h). At higher chamber pressure, the growth rate of the diamond film was decreased due to a massive decrease in the nucleation rate [26]. The pressure dependence concentration of atomic hydrogen near the filament surface has been discussed by Schwarz *et al.* [22] and Schäfer *et al.* [28].

Brunsteiner *et al.* [26] investigated the dependence of the growth rate on chamber pressure and found the maximum growth rate of diamond film at a chamber pressure of 2.7 kPa and a slightly lower growth rate at a chamber pressure of 0.7 kPa. The results of Brunsteiner *et al.* [26] contradict the growth rates of carbon films found in the results of Schwarz *et al.* [22]. The growth rate and quality of diamond at atmospheric pressure (1059.1 kPa) were better than the chamber pressure of 5.0 kPa [29].

3.3. Raman Spectroscopic Analyses of the Carbon Films

In different Raman spectra of the deposited carbon films, the recorded intensity of the Raman signals reveals the morphology and structure of tiny grains, grains, and particles. The presence of the Raman peak near wave number 1332.1 cm^{-1} corresponds to the diamond peak, as shown in Figure 3. In Figure 3, the prominent peak shows different trends and features of the deposited carbon films due to varying chamber pressure.

In Figure 3, a slight shift in the peak is due to the associated stress of the carbon film. The Raman line width varies from the mode of the deposited diamond, which has been discussed related to the degree of structural order [30]. A wavenumber 1581 cm^{-1} , an additional peak was originated. It is related to the G-peak, which is declared due to the highly orientated graphitic phase in CVD diamond coatings [31]. A review study on Raman spectroscopy was discussed by Ferrari and Robertson, studying the structural composition of carbon films [32].

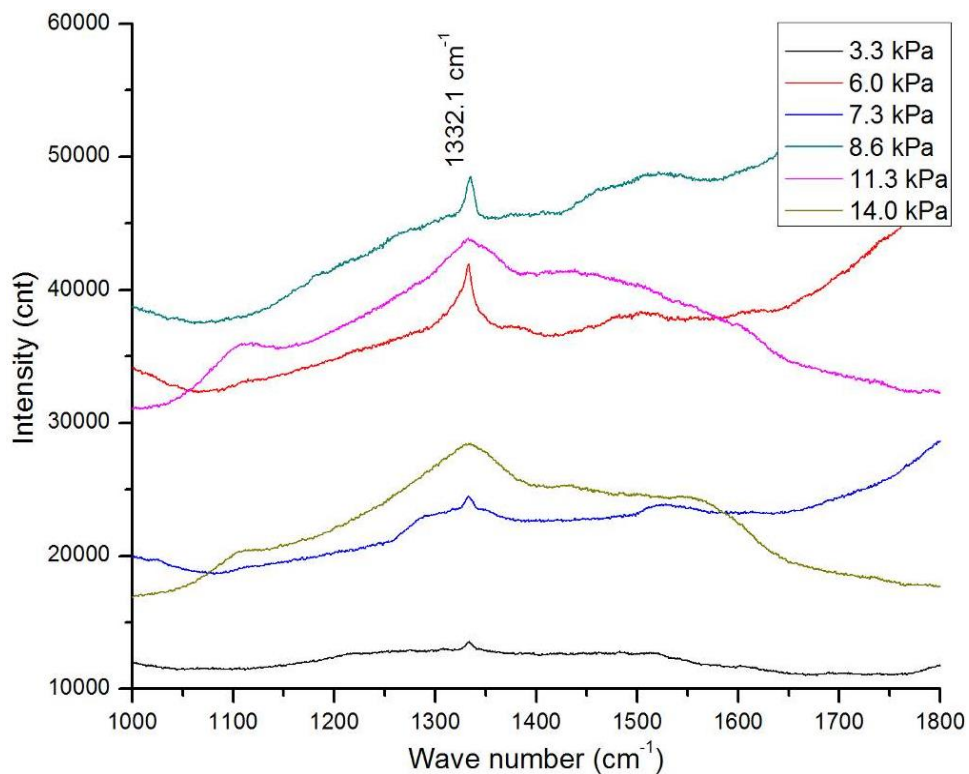


Figure 3: Raman spectra of carbon films deposited at different chamber pressures

Different carbon films synthesized at different chamber pressures remained sensitive to the energy signals of the laser beam, as shown in Figure 3. A pronounced peak at

wave number 1100 cm^{-1} is found in the carbon films deposited at chamber pressures of 11.3 kPa and 14.0 kPa, indicating the presence of a high graphitic phase. A minor signature of this peak also exists for the carbon films deposited at other chamber pressures. Bands and peaks in the results of Raman spectroscopy can be deconvoluted for better relevance. However, more work is required to explore spectroscopic analyses.

3.4. Some Aspects of Nucleation and Growth Mechanisms of Carbon Films

According to the kinetic theory of gases, the mean free path of active species is inversely proportional to the pressure. As there is an enhancement in the chamber pressure, the mean free paths of active species also shorten. Thus, when the carbon atoms deposit in the graphite state, they can detach from the substrate surface. In some cases, graphite state atoms might not adhere to the seeded species or might not trap in the variable regions of the substrate. There is a probability of detachment of those graphite state atoms from the substrate, so nucleation of tiny-sized grain either in graphite state atoms or in diamond state atoms starts from good sites of the seeded and scratched substrate. It indicates that depositing carbon atoms in different states by fully covering the substrate is a grand challenge.

In the hot-filaments reactor, each process deals with a fluctuation of parameters at the start of the process. It is mainly due to the access to set conditions of the process. Again, fluctuation in parameters can be due to the water circulation, or it can be due to the change in the positions of filaments. Different time duration is spent at different chamber pressures to adjust the set value. It can influence the initially nucleating layer of the carbon film. So, a different time duration to achieve set chamber pressure can cause a different nucleation rate. Again, the nature and the condition of the substrate also contribute to controlling the nucleation rate.

Having solved various mathematical equations, Lee *et al.* [17] predicted that the concentration of active species first increases exponentially and finally decreases by decreasing the pressure. Thus, the active species lose the gained energy due to different sorts of collisions at higher pressure. The carbon atoms, which survive, reach the substrate surface to deposit. So, carbon atoms, which do not position to deposit at the substrate surface, either become part of the drain or contaminate the process of

nucleating tiny-sized grains. The nucleation of tiny-sized grains depends on the rate of etching photon energy near the filaments or near the substrate. The nucleation of tiny-sized grains also depends on the rate of releasing typical energy from the gas collision. To keep the same nucleation rate in depositing carbon films is a great challenge.

An increase in the mean free path leads to the partial control of the dynamics in the depositing carbon atoms. It is mainly in the case of low chamber pressures. Hence, the carbon film deposited at a chamber pressure of 3.3 kPa shows a mixed trend. In the mixed trend of the process, a deposited carbon film keeps the growth partially diamond-specific and partially graphite-specific.

The temperature of the filaments decreases at high chamber pressure, as shown in Table 1, under fixed input power. As there is no separate heater to heat the substrate, the substrate temperature also decreases. It is a cause of enhancement of the secondary nucleation. Thus, the thickness of the deposited carbon films reduces. It is also shown in Figure 2 (E) and Figure 2 (F). Figure 2 (D) shows that the carbon film thickness deposited at a chamber pressure of 8.6 kPa remains the highest. The dissociation of molecular hydrogen into atomic hydrogen increases when chamber pressure increases to 8.6 kPa. More gaseous carbon atoms convert into diamond state atoms. However, the rate of dissociating atomic hydrogen is reduced by increasing the chamber pressure to 11.3 kPa or 14.0 kPa. As a result, gaseous carbon atoms convert into graphite state atoms at a low rate. So, carbon atoms are converted into diamond state atoms at a low rate. The growth rates of carbon films decrease along with the deteriorating quality of the diamond content.

Under the commonly employed conditions of the HF-CVD process, the transportation of atomic hydrogen for the growing surface is a diffusion-limited process [33]. Heimann *et al.* [20] observed that the non-diamond content in the films is high at the minimum pressure (0.8 kPa) and high pressure (40 kPa); however, it is low in the film synthesized at a chamber pressure of 20 kPa. Diamond coatings show good quality in reducing the secondary nucleation, where opening the range of pressure increases the option to deposit films in low and high growth rates [22]. Carrying out diamond crystallization in the CVD process [34]. The growth of diamond is a sliding scale between atomic hydrogen and hydrocarbon radical, where only different growth

conditions serve to fix the film morphology and growth rate [35]. Substrate temperature and pressure jointly influence the growth rate of diamond films [36].

At high chamber pressures, dissociation of methane into carbon atoms is high compared to the low and intermediate chamber pressures. However, dissociated carbon atoms frustrate as a sufficient amount of carbon atoms remain in the gaseous state. So, the depositing rate of carbon atoms in the graphite state atoms becomes low. Again, under the low temperature of filaments and substrate, the probability of the required rate of energy coming near the substrate surface also becomes lower, so gaseous carbon atoms convert into graphite state atoms at a lower rate. Consequently, the rate of converting carbon atoms into diamond state atoms becomes low.

The incoming gases reside inside the chamber at increased chamber pressure for a more significant period. Gases residing for a more significant period inside the chamber lower the rate of converting gaseous carbon atoms into diamond state atoms. At increased chamber pressure, the temperature of the filaments is also decreased. Different amounts of typical energy shapes are found inside the deposition reactor at different chamber pressures. Thus, gaseous carbon atoms convert into graphite state atoms and diamond state atoms at different rates. Graphite state atoms bind by the same involved energy, whereas a different shaped typical energy is involved in the binding of diamond state atoms. To deposit carbon films by the HF-CVD system, the study of the mean residence time of gases is also critical [2, 29].

3.5. Growth Rate versus Chamber Pressure

Growth rates of diamond and graphite-specific content are drawn in estimation, shown in Figure 4, at different chamber pressures. The estimated zone of the depositing carbon film at a nearly equal growth rate of diamond and graphite is also labeled by (1) in Figure 4. The maximum growth rate is noted at the chamber pressure of 8.6 kPa, labeled by (2) in Figure 4. The maximum growth rate in graphite is noted at the chamber pressure of 14.0 kPa, labeled by (3) in Figure 4.

At low chamber pressure, which is 3.3 kPa, the dynamics of carbon atoms work in different manners. Some tiny grains grow in the size of the particle, and some do not. Many gaseous carbon atoms get converted into diamond state atoms at intermediate

chamber pressures, 7.3 kPa and 8.6 kPa. Grains and particles were mainly formed in the faceted faces by keeping the high growth rate of the carbon films.

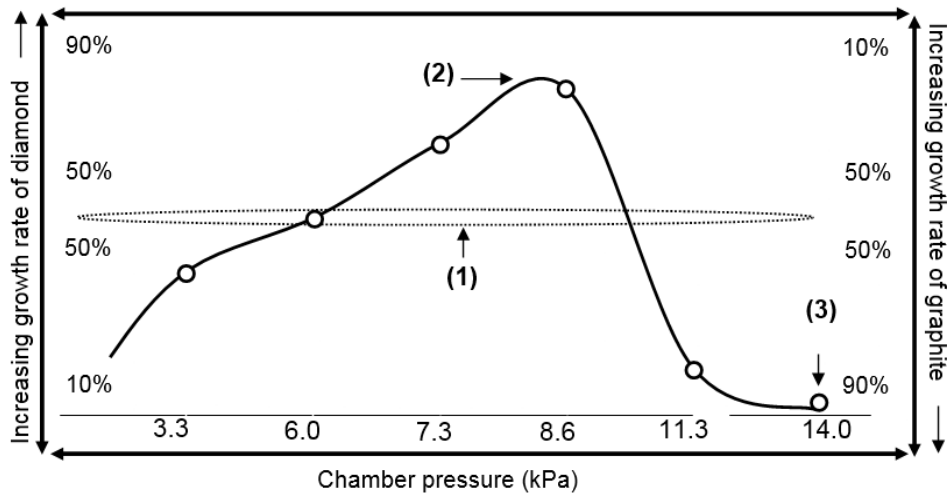


Figure 4: Growth rates of diamond and graphite in the carbon films deposited at varying chamber pressure; **(1)** a zone of balanced (or equal) growth rates of diamond and graphite, **(2)** a zone of the high growth rate of diamond and **(3)** a zone of the high growth rate of graphite

At high chamber pressures, the morphology of grains and particles develops in the dome shape. However, the growth rates of carbon films are low. The gaseous carbon atoms mainly get converted into the graphite content. At 11.3 kPa, the morphology of grains is more like the dome shape. On increasing the chamber pressure up to 14.0 kPa, the morphology of grains is again like the dome shape. At high chamber pressures, tiny grains or grains or particles are mainly related to the graphitic phase.

The graphitic phase in the deposited carbon films is low at low chamber pressures. The graphitic phase in the deposited carbon films is further lower at intermediate chamber pressures. The growth rate of diamond in deposited carbon film is dominant at the intermediate chamber pressures and the least dominant at the high chamber pressures. At high chamber pressures, locally engaged forces synchronize to preserve the typical energy required to form tiny grains, grains, and particles with a graphitic structure. However, locally engaged forces synchronize at intermediate chamber pressures to preserve the typical energy required to form tiny grains and diamond structures.

3.6. Dissociation of H₂ and CH₄ Gases – A Gas Activation Process

The rate of dissociation of H₂ gas and the rate of dissociation of CH₄ gas together determine the gas activation process. In the HF-CVD reactor, molecules of methane and hydrogen dissociate for conversion into the atomic states. Molecular hydrogen converts into hydrogen atoms under the thermal activation of hot filaments. In converting the methane molecule into the carbon component and the four hydrogen atoms, the hydrogen atoms detach from the binding states of the carbon atom. On detachment of the four hydrogen atoms, the binding states of a carbon atom become unfilled, enabling its conversion to either graphite state atom or diamond state atom.

In the dissociation of the CH₄ molecule, expansion and contraction behaviors of two different natures are triggered, where the carbon component gives away four hydrogen atoms. In this way, CH₄ converts into a carbon component and four hydrogen atoms. In the process of dissociation of the CH₄ molecule, four hydrogen atoms separate at the same time. However, a hydrogen molecule requires activation energy up to a higher level to convert into hydrogen atoms. The resulted amounts of hydrogen atoms are being used to etch the photon energy into typical energy. A study on diamond films discusses the temperature of hot filaments in the deposition [37].

The rate of dissociating molecular hydrogen into the atomic hydrogen is varied at different chamber pressures. Again, the rate of converting methane molecules into gaseous carbon and hydrogen atoms becomes different under the varying chamber pressure. The gas activation process varies at different chamber pressures. The rate of etching photon energy also varies under varying chamber pressure.

There is a need to study the dissociation rate of H₂ and CH₄ gases at varying chamber pressure. Again, to find out the different species of gas activation process at different chamber pressures, there is also a need to study the optical emission spectra. Some other qualitative and quantitative analyses can be employed to investigate the rate of gas dissociation and the gas activation process.

3.7. Etching of Photon Energy into Dash and Golf-stick Shaped Typical Energy

From the photon having a short length, typical etched energy shaped like a dash is shown in Figure 5 (a). In Figure 5 (a), two-dotted lines indicate the etching of a photon

by two hydrogen atoms. Typical etched energy shaped like a parabola from the photon having a short length is shown in Figure 5 (b). In Figure 5 (b), the single-dotted line indicates the etching of a photon by one hydrogen atom. Parabola-shaped typical energy is further etched into typical energy shaped like a golf stick in Figure 5 (b).

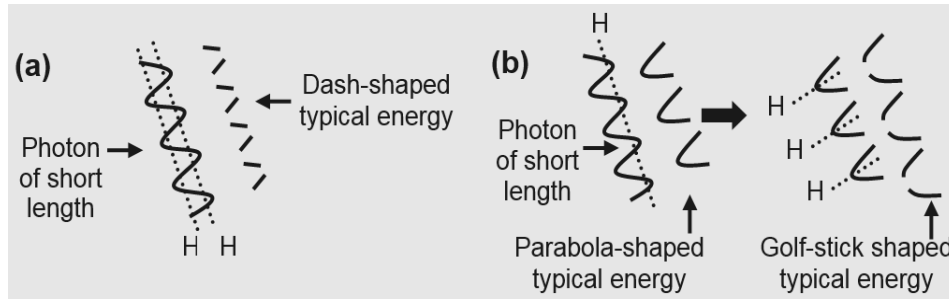


Figure 5: Etching of short-length photon into the (a) dash-shaped typical energy and (b) parabola-shaped typical energy and further etching of the parabolas into the golf-stick shaped typical energy

For different chamber pressures, the etching of photon energy is varied. A different amount of atomic hydrogen is produced for each set chamber pressure. Therefore, a different amount of photon energy is being etched by the atomic hydrogen. The etching of photon energy into dash-shaped typical energy is varied at each set chamber pressure, and the same is the case for typical energy having a shape like a golf stick.

Two pieces of typical energy shaped like a dash involve transferring the electrons to convert the carbon atom into another state [38]. Gaseous carbon atoms get converted into graphite and diamond state atoms in the region close to the hot filaments. So, the typical energy shaped like a dash is primarily produced near the filaments. The distance between the substrate and hot filaments is a few millimetres. The suitable interaction of atomic hydrogen can further etch the typical etched energy shaped like a parabola. In this way, the shape of new typical energy becomes like a golf stick. In the diamond structure, atoms bind by the involvement of golf-stick typical energy [38].

Filaments deal with photonic current. In the deposition chamber, hot-filaments release the photons of short and long lengths called overt photons. Photons released from the hot filaments are the source of different pieces of typical energy. Photons are being etched by the atomic hydrogen converting into different shapes of typical energy. Under the etching of atomic hydrogen, a photon is etched into the pieces of typical

energy, having the shape of a dash, parabola, and golf stick. A separate study has detailed the photon study [39].

3.8. Gas Collision and Arrival of Typical Energy

The rate of etching energy into golf-stick-shaped typical energy increases on increasing the chamber pressure and decreases on further increasing the chamber pressure. The trend is plotted in estimation in Figure 6 (a) – a plot in a solid curve. The rate of etching photon energy into dash-shaped typical energy is moderate at the lowest chamber pressure, low at intermediate chamber pressures, and high at high chamber pressures. This kind of trend is plotted, in estimation, in Figure 6 (b) – a plot in a dotted curve.

In (1) of Figure 6 (a), an approximately drawn point of gas collision is shown by the blue dotted line, which indicates the minimum disruption in the formation of typical energy shaped like (a parabola and) golf-stick. Therefore, gas collision is more favorable at intermediate chamber pressures to release typical energy shaped like a golf stick. Hence, carbon films have a higher growth rate than the diamond phase.

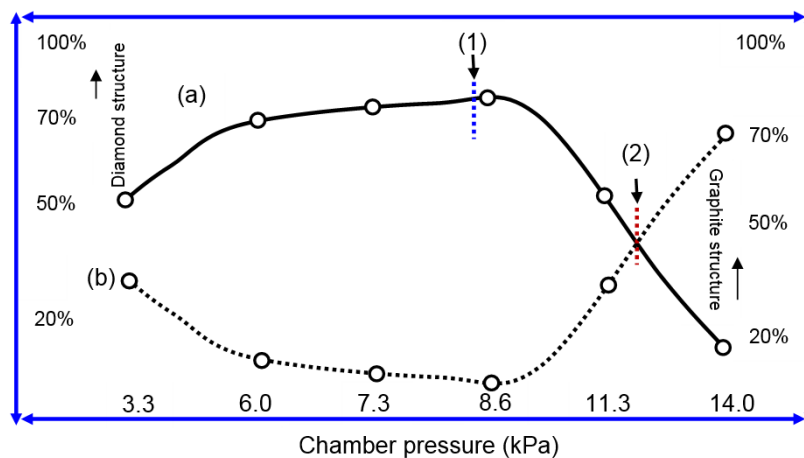


Figure 6: (a) pressure-dependent growth showing point of gas collision having the minimum disruption in coming typical energy to bind (1) diamond atoms. (b) Pressure dependent growth showing the point of a gas collision having the minimum disruption in typical energy coming to bind atoms of (2) graphite

In a gas collision, atomic hydrogen and gaseous carbon are involved, but molecular hydrogen and methane are also involved. The collision rate of gases varies largely at varying chamber pressure, shown in Figure 6 in estimation. However, the collision rate of different gases should first depend on the process of gas activation.

Gas collision is less favorable at high chamber pressures to release the typical energy shaped like a golf stick. However, gas collision is favorable to release typical energy shaped like dash. In (2) of Figure 6 (b), the red-dotted line shows an approximately drawn point of gas collision, which shows the minimum disruption in the formation of typical energy shaped like a dash. In this context, further research is required to understand the gas collision process at different chamber pressures.

Many photons are not found inside the deposition chamber at high chamber pressures. It is due to the excessive contamination of filaments. The lower amount of molecular hydrogen was converted into atomic hydrogen. So, the conversion of atomic hydrogen remained at a lower rate. Thus, the rate of converting gaseous carbon atoms into diamond state atoms remained minimum. Again, high chamber pressures deal with the more dissipation of heat energy instead of dealing with the more releasing of photon energy. The presence of heat energy inside the reactor affects the process.

3.9. General Discussion

In studies given elsewhere [2, 9], the role of atomic hydrogen remained crucial in determining the content-specific growth of a carbon film. Increasing a small amount of CH₄ in the total mass flow rate lowers the quality of diamond film [2]. The carbon film deposited at a single substrate grew with higher diamond composition when the inter-wire distance was kept less [9]. Such studies validate the crucial role of the gas collision. In the HF-CVD system under the existing setting, a low rate of converting gaseous carbon atoms into other states of carbon can be expected.

In Figures 2 (c) and 2 (d), the tilted microscopic images show the pyramid-shaped morphology of large diamond crystallites. Many diamond crystallites are grown by retaining their roots in contact with the substrate surface. In the growth of each diamond crystal, a large number of gaseous carbon atoms got converted into diamond state atoms. Therefore, these carbon films are related to more diamond-specific growth. The growth behavior of grains and particles shown in Figure 2 (c) is almost identical to the growth behavior of grains and particles shown in Figure 2 (d). In Figure 2 (d), the growth of large crystallites can be observed. Such kind of growth behavior discloses the

stinging nature of diamonds. Diamond growth is south to ground, but the structure of diamond is tetra-electron ground to south topological structure [38].

Under different arrangements of hot filaments, the growth rate of the carbon film may differ from the one discussed here. Again, the growth rate of a carbon film can be varied when a different deposition system is employed. To nucleate a tiny grain, the formation of different amounts of typical energy at different chamber pressures can show a different insight. In microwave-based chemical vapor deposition, the structure of tiny grains of carbon films explained the nucleation behavior with some essential detail and how secondary nucleation was initiated [40]. Therefore, much more work is required in the HF-CVD technique to understand the nucleation and growth mechanisms.

The chamber pressure is not the only parameter influencing and defining the entire growth behavior of the carbon films. Several other parameters can also be involved, and some of them are given in Table 1. Filaments and substrate temperature vary at different chamber pressures despite setting the fixed input power. It happened due to varying chamber pressure in the reactor. At different chamber pressures, it is not possible to keep the temperature of filaments constant. The published studies also indicate the approximate values of temperature.

Different chamber designs can lead to the different effects of chamber pressure on the morphology and structure of carbon films. At the same chamber pressure, the arrival rate of typical energy can be varied. The compositions of graphite and diamond quantified in Figures 4 and 6 are based on the results presented in Figures 1, 2, and 3. There is a need to discuss the kinetics, dynamics, mass spectroscopy, computational modeling of gas dissociation, and the gas activation of the process.

4.0. Conclusion

Tiny carbon grains nucleate at different rates for different chamber pressures. At low chamber pressures, the rate of converting gaseous carbon atoms into graphite and diamond state atoms is moderate. At intermediate chamber pressures, gaseous carbon atoms convert into diamond state atoms at a high rate. At high chamber pressures, the rate of converting gaseous carbon atoms into graphite state atoms is high. Nucleations

of the diamonds start at the feasible sites of the roughened substrate. In the carbon film, tiny grains grow, reaching the size of grains and particles.

At 3.3 kPa and 6.0 kPa chamber pressures, a mixed trend of growth behavior is observed in the deposited carbon films. At 7.3 kPa and 8.6 kPa chamber pressures, the morphologies of grains and particles mainly develop in the pyramid shape related to diamonds. At 11.3 kPa and 14.0 kPa chamber pressures, the morphologies of grains and particles primarily develop in the dome shape, which is related to graphite. The thickness of the carbon films depends on the rate of converting carbon atoms into a diamond state or graphite state.

In different carbon films, the morphologies of grains and particles are sensitive to the Raman signals giving information about their shapes. Grains and particles show high purity diamond-wise at chamber pressures 6.0 kPa, 7.3 kPa, and 8.6 kPa, whereas high purity graphite-wise at chamber pressures 11.3 kPa and 14.0 kPa. X-ray analyses of the carbon films deposited at varying chamber pressures agree with the information provided by the spectroscopic analysis and FE-SOM investigation.

Dissociating CH_4 molecules and molecular hydrogen varies at different chamber pressures. A CH_4 molecule simultaneously dissociates into a carbon atom and four hydrogen atoms, and a hydrogen molecule dissociates into the atomic hydrogen under the thermal activation of the hot filaments. The rate of dissociation of gases determines the gas activation process. The rate of the gas activation process determines the gas collision process.

The hot filaments release the photons at different rates at different chamber pressures. Dissociated hydrogen atoms shape the photon energy into the typical energy. Due to the varying gas activation and gas collision processes at each chamber pressure, the amount of photon energy etched into typical energy is also varied. The required amount of typical energy changing the rate of converting gaseous carbon atoms into graphite and diamond state atoms is related to the rate of dissociating molecular hydrogen.

At different chamber pressures, the gas activation process and the gas collision process influence the rate of binding carbon atoms. At intermediate chamber pressures, more molecular hydrogen dissociates into atomic hydrogen. Thus, typical energy

shaped like parabola and golf-stick form in a more significant amount. At chamber pressures 6.0 kPa, 7.3 kPa, and 8.6 kPa, the gaseous carbon atoms convert into diamond state atoms at a high rate, but the rate of their binding also becomes high.

Dash-shaped typical energy converts gaseous carbon atoms into another state, graphite state atoms bind under the same energy, but golf-stick-shaped typical energy gets involved in the binding diamond state atoms [38]. At intermediate chamber pressures, a gas collision process favors the etching of photon energy, so typical energy shaped like a golf stick produces a more significant amount. The etching of photon energy in the dash shape is high at 11.3 kPa and 14.0 kPa. At 6.0 kPa, 7.3 kPa, and 8.6 kPa, the etching of photon energy in parabola and golf-stick shapes is high. At 3.3 kPa, the etching photon energy in parabola and golf-stick shapes is moderate.

The work provides insight into problem-based solutions. It can enable one to explore cutting-edge technologies. Further, the study helps to discuss the science of semiconductors from a new perspective. There is vast room to synthesize carbon films with different applications in the hot-filaments reactor. New designs of the deposition systems can provide opportunities to synthesize carbon films with better performances. In new depositions, resource utilization can minimize, leading to the building of a clean environment.

Acknowledgments:

Mubarak Ali expresses sincere gratitude to The Scientific and Technological Research Council of Turkey (TÜBİTAK), the letter ref. # B.02.1.TBT.0.06.01-216.01-677-6045 for honoring postdoc award (year 2010). The authors thank Mr. Talat ALPAK (ITU, Istanbul) for helping in the field emission scanning microscope. Mubarak Ali appreciates the kind support of Professor Dr. Kürşat KAZMANLI, Dr. Erdem Arpat, Dr. Semih ÖNCEL, Dr. Manawer, and Dr. Nagihan Sezgin, Dr. Sinan Akkaya, and others while staying at ITU, Turkey.

Data Availability Statement:

All data generated or analyzed during this study are included in this published article.

Conflicts of Interest:

The authors declare no conflicts of interest.

References

- [1] C. Yan, Y. K. Vohra, H. Mao, R. J. Hemley, Very high growth rate chemical vapor deposition of single-crystal diamond, *Proc. Natl. Acad. Sci. U.S.A* 99 (2002) 12523-12525.
- [2] M. Ali, M. Ürgen, Surface morphology, growth rate and quality of diamond films synthesized in hot filament CVD system under various methane concentrations, *Appl. Surf. Sci.* 257 (2011) 8420-8426.
- [3] M. Ali, M. Ürgen, Growth of in-situ multilayer diamond films by varying substrate-filament distance in hot filament chemical vapor deposition system, *J. Mater. Res.* 27 (2012) 3123-3129.
- [4] M. Ali, M. Ürgen, M. A. Atta, Effect of surface treatment on hot-filament chemical vapour deposition grown diamond films, *J. Phys. D: Appl. Phys.* 45 (2012) 045301-07.
- [5] M. Mertens, M. Mohr, N. Wiora, K. Brühne, H. Fecht, N-Type Conductive Ultrananocrystalline Diamond Films Grown by Hot Filament CVD, *J. Nanomater.* 2015 (2015) 527025.
- [6] M. Ali, M. Ürgen, Switching dynamics of morphology-structure in chemically deposited carbon films –A new insight, *Carbon* 122 (2017) 653-663.
- [7] G. Yan, et al. Mechanical properties and wear behavior of multi-layer diamond films deposited by hot-filament chemical vapor deposition. *Applied Surface Science*, 494 (2019) 401-411.
- [8] R. L. Martins, D. D. Damm, E. J. Corat, V. J. Trava-Airoldi, D. M. Barquete. Mitigating residual stress of high temperature CVD diamond films on vanadium carbide coated steel. *Journal of Vacuum Science & Technology A*, 39 (2021) 013401.
- [9] M. Ali, M. Ürgen, Simultaneous growth of diamond and nanostructured graphite thin films by hot filament chemical vapor deposition, *Solid State Sci.* 14 (2012) 150-154.

- [10] R. Ahmed, et al. Ultraviolet micro-Raman stress map of polycrystalline diamond grown selectively on silicon substrates using chemical vapor deposition. *Applied Physics Letters*, 112 (2018) 181907.
- [11] R. Simões, B. Martins, J. Santos, V. Neto, HFCVD Diamond-Coated Mechanical Seals, *Coatings* 8 (2018) 172.
- [12] N. Yang, et al. Conductive diamond: synthesis, properties, and electrochemical applications. *Chemical Society Reviews*, 48 (2019) 157-204.
- [13] M. Behera, A. Jena, S. K. Pattnaik, S. Padhi, S. K. Sarangi. The effect of transition-metal seeding powder on deposition and growth of diamond synthesized by hot filament chemical vapor deposition processes on cemented carbide substrates and its characterization. *Materials Chemistry and Physics*, 256 (2020) 123638.
- [14] L. Zhang, et al. Highly Oriented Graphitic Networks Grown by Chemical Vapor Deposition as Thermal Interface Materials. *Industrial & Engineering Chemistry Research*, 59 (2020) 22501-22508.
- [15] J. Yu, R. Huang, L. Wen, C. Shi, Effects of density of gas flow rate on large area diamond growth in hot filament chemical vapour deposition, *J. Mater. Sci. Lett.* 17 (1998) 1011-1013.
- [16] J. Zimmer, K. V. Ravi, Aspects of scaling CVD diamond reactors, *Diam. Relat. Mater.* 15 (2006) 229-233.
- [17] S. T. Lee, Y. W. Lam, Z. Lin, Y. Chen, Q. Chen, Pressure effect on diamond nucleation in a hot filament CVD system, *Phys. Rev. B* 55 (1997) 15937-15941.
- [18] J. Kang, C. Xiao, Y. Xiong, Y. Wang, Q. Meng, Z. Lin *et al.*, Diamond nucleation and growth under very low pressure conditions, *Diam. Relat. Mater.* 9 (2000) 1691-1695.
- [19] Z. Yu, A. Flodström, Pressure Dependence of Growth Mode of HFCVD Diamond, *Diam. Relat. Mater.* 6 (1997) 81-84.
- [20] B. Heimann, V. Rako, V. Buck, Search for scaling parameters for growth rate and purity of hot-filament CVD diamond, *Int. J. Refract. Metals Hard Mater.* 19 (2001) 169-175.

- [21] K. K. Hirakuri, T. Kobayashi, E. Nakamura, N. Mutsukura, G. Friedbacher, Y. Machi, Influence of the methane concentration on HF-CVD diamond under atmospheric pressure, *Vacuum* 63 (2001) 449-454.
- [22] S. Schwarz, S. M. Rosiwal, M. Frank, D. Breidt, R. F. Singer, Dependence of the growth rate, quality, and morphology of diamond coatings on the pressure during the CVD-process in an industrial hot-filament plant, *Diam. Relat. Mater.* 11 (2002) 589-595.
- [23] S. K. Sarangi, A. Chattopadhyay, A. K. Chattopadhyay, Effect of pretreatment methods and chamber pressure on morphology, quality and adhesion of HFCVD diamond coating on cemented carbide inserts, *Appl. Surf. Sci.* 254 (2008) 3721–3733.
- [24] S. J. Harris, A. M. Weiner, Pressure and temperature effects on the kinetics and quality of diamond films, *J. Appl. Phys.* 75 (1994) 5026-5032.
- [25] Y. -Z. Wan, D. W. Zhang, Z. -J. Liu, J. -T. Wang, Effects of temperature and pressure on CVD diamond growth from the C-H-O system, *Appl. Phys. A* 67 (1998) 225-231.
- [26] R. Brunsteiner, R. Haubner, B. Lux, Hot-filament chemical vapour deposition of diamond on SiAlON at pressures up to 500 Torr, *Diam. Relat. Mater.* 2 (1993) 1263-1270.
- [27] M. Ali, Qualitative Analyses of Thin Film-Based Materials Validating New Structures of Atoms. (2022) <https://www.researchgate.net/publication/352830671>
- [28] L. Schäfer, C. -P. Klages, U. Meier, K. Kohse-Höinghaus, Atomic hydrogen concentration profiles at filaments used for chemical vapor deposition of diamond, *Appl. Phys. Lett.* 58 (1991) 571-573.
- [29] T. Kobayashi, K. K. Hirakuri, N. Mutsukura, Y. Machi, Synthesis of CVD diamond at atmospheric pressure using the hot-filament CVD method, *Diam. Relat. Mater.* 8 (1999) 1057-1060.
- [30] D. S. Knight, W. B. White, Characterization of diamond films by Raman spectroscopy, *J. Mater. Res.* 4 (1989) 385-393.
- [31] P. K. Chu, L. Li, Characterization of amorphous and nanocrystalline carbon films, *Mater. Chem. Phys.* 96 (2006) 253-277.

- [32] A. C. Ferrari, J. Robertson, Raman spectroscopy of amorphous, nanostructured, diamond-like carbon, and nanodiamond, *Philos Trans A Math Phys Eng Sci*, 362 (2004) 2477-2512
- [33] J. C. Angus, A. Argoitia, R. Gat, Z. Li, M. Sunkara, L. Wang, Y. Wang, Chemical Vapour Deposition of Diamond, *Philos. Trans. R. Soc. A-Math. Phys. Eng. Sci.* 342 (1993) 195.
- [34] W. J. P. van Enckevort, G. Janssen, W. Vollenberg, J. J. Schermer, L. J. Giling, M. Seal, CVD diamond growth mechanisms as identified by surface topography, *Diam. Relat. Mater.* 2 (1993) 997.
- [35] P. W. May, A. Y. Mankelevich, From ultrananocrystalline diamond to single crystal diamond growth in hot filament and microwave plasma-enhanced CVD reactors: a unified model for growth rates and grain sizes, *J. Phys. Chem. C* 112 (2008) 12432.
- [36] J. -G. Zhang, X. -C. Wang, B. Shen, F. -H. Sun, Effect of deposition parameters on micro- and nano-crystalline diamond films growth on WC-Co substrates by HFCVD, *Trans. Nonferrous Met. Soc. China* 24 (2014) 3181.
- [37] Y. Takamori, et al. Insight into temperature impact of Ta filaments on high-growth-rate diamond (100) films by hot-filament chemical vapor deposition. *Diamond and Related Materials*, 118 (2021) 108515.
- [38] M. Ali. Atomic Structure and Binding of Carbon Atoms. (2022), <https://www.preprints.org/manuscript/201801.0036/v12>
- [39] M. Ali, Heat and Photon Energy Phenomena: Dealing with Matter at Atomic and Electronic Level. (2022), <https://www.preprints.org/manuscript/201701.0028/v12>
- [40] M. Ali, I –N. Lin, Phase transitions and critical phenomena of tiny grains carbon films synthesized in microwave-based vapor deposition system, *Surf. Interface Anal.* 51 (2019) 389-399.

Authors' biography:



Mubarak Ali graduated from University of the Punjab with BSc (Phys & Math) in 1996 and MSc in Materials Science with distinction from Bahauddin Zakariya University, Multan, Pakistan (1998); his thesis work was completed at Quaid-i-Azam University Islamabad. He gained a Ph.D. in Mechanical Engineering from the Universiti Teknologi Malaysia under the award of the Malaysian Technical Cooperation Programme (MTCP;2004-07) and a postdoc in advanced surface technologies at Istanbul Technical University under the foreign fellowship of The Scientific and Technological Research Council of Turkey (TÜBİTAK, 2010). Dr. Mubarak completed another postdoc in nanotechnology at the Tamkang University Taipei in 2013-2014, sponsored by National Science Council, now M/o Science and Technology, Taiwan (R.O.C.). Presently, he is working as an Assistant Professor on the tenure track at COMSATS University Islamabad (previously known as COMSATS Institute of Information Technology), Islamabad, Pakistan (since May 2008, and the position renewal is in the process) and before that, worked as assistant director/deputy director at M/o Science & Technology (Pakistan Council of Renewable Energy Technologies, Islamabad, 2000-2008). The Institute for Materials Research, Tohoku University, Japan, invited him to deliver a scientific talk. He gave several scientific talks in various countries. His core area of research includes materials science, physics & nanotechnology. He was also offered a merit scholarship for the Ph.D. study by the Higher Education Commission, Government of Pakistan, but he did not avail himself of the opportunity. He earned a diploma (in English) and a certificate (in the Japanese language) in 2000 and 2001, respectively, part-time from the National University of Modern Languages, Islamabad. He is the author of several articles available at the following links;
https://www.researchgate.net/profile/Mubarak_Ali5 &
<https://scholar.google.com.pk/citations?hl=en&user=UYjvhDwAAAAJ>



Mustafa Ürgen graduated from Istanbul Technical University in 1977, Mining Faculty, followed by his M.Sc. from Metallurgical Engineering Faculty in 1978 and Ph.D. from Institute of Science and Technology in 1986. He remained a visiting fellow at Max-Planck Institut, Institut für Metallwissenschaften, Stuttgart, Germany (1988-89) and won the IMF award – Jim Kape Memorial Medal in 1998, London, UK. He is one of the top grants winning senior standing professors of the Istanbul Technical University. Professor Ürgen is head of several laboratories in diversified areas of science & technology (Surface Technologies: Electrolytic and conversion coatings, diffusion coating techniques, vacuum coating techniques, PVD coatings, composite coatings, surface analysis. Corrosion and Corrosion Protection: Mechanism of corrosion reactions, pitting corrosion (stainless steel, aluminum alloys, ceramic, DLC coated metals), stress corrosion cracking. He worked at several managerial and administrative positions at departmental, faculty, and university levels and supervised several Ph.D. and postdoc candidates funded locally and internationally, and some of his students are working as full professors. Professor Ürgen delivered many talks at various forums to his credit. He secured commercialized patents and a long list of publications in refereed journals on diversified classes of materials, physics and chemistry, and other interdisciplinary areas of science and technology. Prof. Ürgen is the author of several articles available at links; <https://scholar.google.com/citations?user=3TEIpuUAAA&hl=en> and https://www.researchgate.net/profile/Mustafa_Urgen